

# Arteriosclerosis, Thrombosis, and Vascular Biology



JOURNAL OF THE AMERICAN HEART ASSOCIATION

## Depolarization of Mitochondria in Endothelial Cells Promotes Cerebral Artery Vasodilation by Activation of Nitric Oxide Synthase

Prasad V.G. Katakam, Edina A. Wappler, Paige S. Katz, Ibolya Rutkai, Adam Institoris, Ferenc Domoki, Tamás Gáspár, Samuel M. Grovenburg, James A. Snipes and David W. Busija

*Arterioscler Thromb Vasc Biol.* 2013;33:752-759; originally published online January 17, 2013;  
doi: 10.1161/ATVBAHA.112.300560

*Arteriosclerosis, Thrombosis, and Vascular Biology* is published by the American Heart Association, 7272  
Greenville Avenue, Dallas, TX 75231

Copyright © 2013 American Heart Association, Inc. All rights reserved.  
Print ISSN: 1079-5642. Online ISSN: 1524-4636

The online version of this article, along with updated information and services, is located on the  
World Wide Web at:

<http://atvb.ahajournals.org/content/33/4/752>

Data Supplement (unedited) at:

<http://atvb.ahajournals.org/content/suppl/2013/01/17/ATVBAHA.112.300560.DC1.html>

<http://atvb.ahajournals.org/content/suppl/2013/01/22/ATVBAHA.112.300560.DC2.html>

**Permissions:** Requests for permissions to reproduce figures, tables, or portions of articles originally published in *Arteriosclerosis, Thrombosis, and Vascular Biology* can be obtained via RightsLink, a service of the Copyright Clearance Center, not the Editorial Office. Once the online version of the published article for which permission is being requested is located, click Request Permissions in the middle column of the Web page under Services. Further information about this process is available in the [Permissions and Rights Question and Answer](#) document.

**Reprints:** Information about reprints can be found online at:

<http://www.lww.com/reprints>

**Subscriptions:** Information about subscribing to *Arteriosclerosis, Thrombosis, and Vascular Biology* is online at:

<http://atvb.ahajournals.org/subscriptions/>

# Depolarization of Mitochondria in Endothelial Cells Promotes Cerebral Artery Vasodilation by Activation of Nitric Oxide Synthase

Prasad V.G. Katakam, Edina A. Wappler, Paige S. Katz, Ibolya Rutkai, Adam Institoris, Ferenc Domoki, Tamás Gáspár, Samuel M. Grovenburg, James A. Snipes, David W. Busija

**Objective**—Mitochondrial depolarization after ATP-sensitive potassium channel activation has been shown to induce cerebral vasodilation by the generation of calcium sparks in smooth muscle. It is unclear, however, whether mitochondrial depolarization in endothelial cells is capable of promoting vasodilation by releasing vasoactive factors. Therefore, we studied the effect of endothelial mitochondrial depolarization by mitochondrial ATP-sensitive potassium channel activators, BMS-191095 (BMS) and diazoxide, on endothelium-dependent vasodilation.

**Approach and Results**—Diameter studies in isolated rat cerebral arteries showed BMS- and diazoxide-induced vasodilations that were diminished by endothelial denudation. Mitochondrial depolarization-induced vasodilation was reduced by inhibition of mitochondrial ATP-sensitive potassium channels, phosphoinositide-3 kinase, or nitric oxide synthase. Scavenging of reactive oxygen species, however, diminished vasodilation induced by diazoxide, but not by BMS. Fluorescence studies in cultured rat brain microvascular endothelial cells showed that BMS elicited mitochondrial depolarization and enhanced nitric oxide production; diazoxide exhibited largely similar effects, but unlike BMS, increased mitochondrial reactive oxygen species production. Measurements of intracellular calcium ( $[Ca^{2+}]_i$ ) in cultured rat brain microvascular endothelial cells and arteries showed that both diazoxide and BMS increased endothelial  $[Ca^{2+}]_i$ . Western blot analyses revealed increased phosphorylation of protein kinase B and endothelial nitric oxide synthase (eNOS) by BMS and diazoxide. Increased phosphorylation of eNOS by diazoxide was abolished by phosphoinositide-3 kinase inhibition. Electron spin resonance spectroscopy confirmed vascular nitric oxide generation in response to diazoxide and BMS.

**Conclusions**—Pharmacological depolarization of endothelial mitochondria promotes activation of eNOS by dual pathways involving increased  $[Ca^{2+}]_i$  as well as by phosphoinositide-3 kinase-protein kinase B-induced eNOS phosphorylation. Both mitochondrial reactive oxygen species-dependent and -independent mechanisms mediate activation of eNOS by endothelial mitochondrial depolarization. (*Arterioscler Thromb Vasc Biol.* 2013;33:752-759.)

**Key Words:** BMS-191095 ■ diazoxide ■ intracellular calcium ■ membrane potential ■ mitochondrial ATP-sensitive potassium channels ■ superoxide

Mitochondria appear to play an important role in the regulation of cerebral vascular tone. Recent, limited evidence shows that mitochondria-derived factors promote relaxation of intact or endothelium-denuded cerebral arteries or isolated vascular smooth muscle (VSM) cells.<sup>1-4</sup> Mitochondrial depolarization in VSM with diazoxide, an activator of mitochondrial ATP-sensitive potassium (mito- $K_{ATP}$ ) channels, promotes the generation of reactive oxygen species (ROS) from mitochondria, which sequentially causes the activation of ryanodine-sensitive  $Ca^{2+}$  channels on sarcoplasmic reticulum, generation of calcium transients, otherwise known as calcium sparks, and the opening of adjacent large-conductance calcium-activated potassium channels ( $BK_{Ca}$ ) on the plasma membrane. The efflux of  $K^+$  thus leads to

hyperpolarization, decreased global intracellular  $Ca^{2+}$  of VSM, and vasodilation.<sup>1,2</sup> However, the contribution of endothelium to the integrated cerebral arterial response to mitochondrial depolarization as well as to other potential mechanisms has never been systematically investigated.

## See accompanying editorial on page 673

Our laboratory has provided physical and pharmacological evidence that selective mitochondrial depolarizing agents promote endothelium-dependent vasodilation/vasoconstriction by inducing the release of factors such as nitric oxide and constrictor prostaglandins, which modulate VSM effects in cerebral arteries.<sup>3</sup> However, the precise mechanisms by which endothelial mitochondrial depolarization promotes

Received on: May 21, 2012; final version accepted on: December 17, 2012.

From the Department of Pharmacology, Tulane University School of Medicine, New Orleans, LA (P.V.G.K., E.A.W., P.S.K., I.R., S.M.G., D.W.B.); Department of Physiology and Pharmacology, Wake Forest University Health Sciences, Winston Salem, NC (P.V.G.K., E.A.W., A.I., F.D., T.G., J.A.S., D.W.B.); and Department of Physiology, University of Szeged School of Medicine, Szeged, Hungary (A.I., F.D.).

The online-only Data Supplement is available with this article at <http://atvb.ahajournals.org/lookup/suppl/doi:10.1161/ATVBAHA.112.300560/-DC1>. Correspondence to Prasad V.G. Katakam, MD, PhD, Department of Pharmacology, Tulane University School of Medicine, 1430 Tulane Avenue, New Orleans, LA 70112. E-mail [pkatakam@tulane.edu](mailto:pkatakam@tulane.edu)

© 2013 American Heart Association, Inc.

*Arterioscler Thromb Vasc Biol* is available at <http://atvb.ahajournals.org>

DOI: 10.1161/ATVBAHA.112.300560

endothelium-dependent vasodilation cannot be elucidated from previous studies. The ability of endothelial mitochondrial depolarization to affect cerebrovascular tone is a novel and potentially important area of investigation, as many physiological, pharmacological, pathological, and physical factors impacting endothelium has been shown in other regional circulations,<sup>5-11</sup> but not yet in the cerebral circulation.

Two relatively selective openers of mitoK<sub>ATP</sub> channels, diazoxide and BMS-191095 (BMS), are available, and we have studied their properties extensively in isolated mitochondria, cultured neurons, and astrocytes.<sup>12-16</sup> Although both depolarize mitochondria, diazoxide, but not BMS, causes increased production of ROS from mitochondria presumably by inhibiting succinate dehydrogenase.<sup>17</sup> We<sup>12,13,16</sup> and others<sup>18-21</sup> are unaware of any effects of BMS other than as an opener of mitoK<sub>ATP</sub> channels. No previous studies have examined the effects of BMS on cerebral arterial tone, and the endothelium-specific effects of diazoxide have not been specifically studied. In this study, we examined the effect of mitochondrial depolarization in endothelium on integrated cerebral vascular tone and explored the mechanisms involved. Our results have allowed us to document the key elements of signaling steps that link mitochondrial depolarization with the generation of nitric oxide (NO) by cerebral vascular endothelium, including activation of endothelial nitric oxide synthase (eNOS) by dual pathways involving increased [Ca<sup>2+</sup>]<sub>i</sub> as well as by phosphoinositide 3-kinase (PI3K)-protein kinase B (Akt)-induced phosphorylation.

## Results

### Intraluminal Diameter Measurements

The resting diameters of the cerebral arteries were similar for each group of experiments (169±4, n=91, in endothelium-intact and 163±4, n=19, in endothelium-denuded; *P*=NS), and they were precontracted to a similar degree (52±1, n=34, in endothelium-intact and 51±2, n=14, in endothelium-denuded; *P*=NS). The BMS elicited a dose-dependent vasodilation in cerebral arteries with 16.3±1.4%, 49.7±4.7%, and 62.6±4.4% relaxation in response to 10, 50, and 100 μmol/L, respectively (n=6-12). Similarly, diazoxide elicited a dose-dependent vasodilation with 8.9±1.2%, 21.9±2.9%, and 39.5±2.8% relaxation in response to 10, 50, and 100 μmol/L,

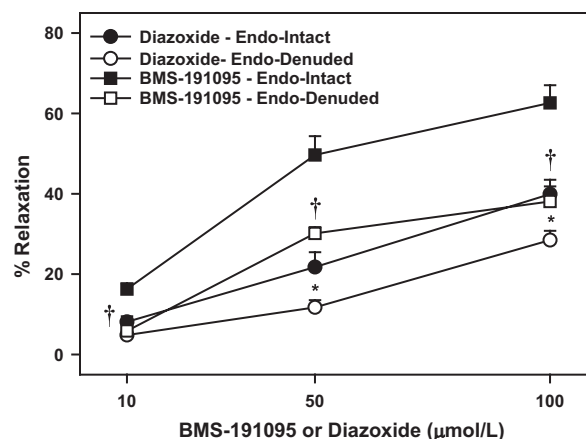


**Figure 1.** Responses to BMS-191095 (BMS) and diazoxide (10, 50, and 100 μmol/L) in endothelium-intact and -denuded cerebral arteries from Sprague Dawley (SD) rats after development of myogenic tone are shown. Data are mean±SEM of 6 to 14 experiments. \* and † indicate significant difference in corresponding response in endothelium-intact arteries with respect to BMS and diazoxide, respectively (*P*<0.05).

respectively (n=10; Figure 1). Denudation of endothelium diminished vasodilation to BMS with 5.9±0.9%, 31.6±2.1%, and 38.1±3.8% relaxation in response to 10, 50, and 100 μmol/L, respectively (n=10; *P*<0.05). Similarly, denudation of endothelium diminished vasodilation to diazoxide with 4.8±1.3%, 11.7±3.5%, and 28.5±2.3% relaxation in response to 10, 50, and 100 μmol/L, respectively (n=9; *P*<0.05; Figure 1). Thus, endothelium contributes to vasodilation in response to both BMS and diazoxide.

Scavenging of the ROS with MnTBAP did not affect vasodilation to BMS (51.1±4.3, n=5; *P*=NS) confirming that BMS-induced vasodilation was independent of ROS generation (Figure 2A). In contrast, MnTBAP diminished vasodilation to diazoxide (8.6±1.3, n=5; *P*<0.05) confirming that diazoxide-induced vasodilation was ROS-dependent (Figure 2B). Inhibition of mitoK<sub>ATP</sub> channels alone with 5-hydroxydecanoic acid (11.7±2%, n=14; *P*<0.05) and fluoxetine (19.5±4%, n=5; *P*<0.05), or both mitochondrial and plasma membrane K<sub>ATP</sub> with glibenclamide (22.3±4%, n=6; *P*<0.05) decreased vasodilation to BMS in endothelium-intact arteries (Figure 2A). Wortmannin pretreatment

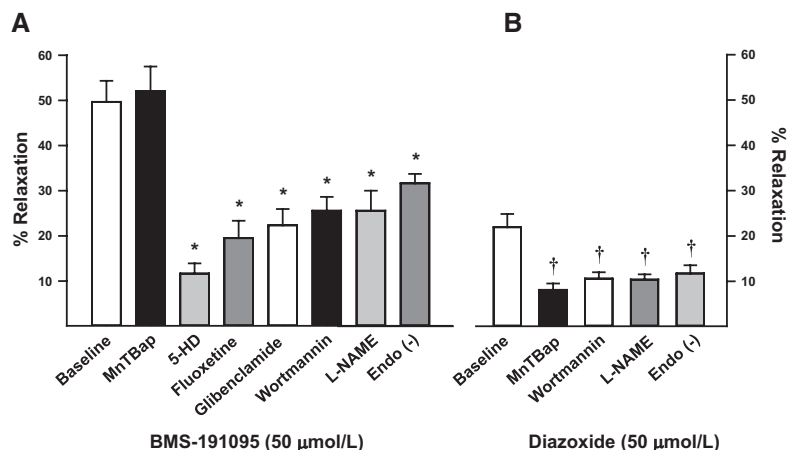


**Figure 2.** Vascular responses to 50 μmol/L BMS-191095 (A) and diazoxide (B) in endothelium-intact rat cerebral arteries in the presence and absence of 100 μmol/L manganese(III) tetrakis(4-benzoic acid)porphyrin chloride (MnTBAP), 1 mmol/L 5-hydroxydecanoic acid (5-HD), 5 μmol/L fluoxetine, 10 μmol/L glibenclamide, 100 nmol/L wortmannin, and 100 μmol/L N<sup>ω</sup>-nitro L-arginine methyl ester (L-NAME) are shown as bar graphs. In addition, vascular responses to 50 μmol/L BMS-191095 and diazoxide in endothelium-denuded rat cerebral arteries are also displayed in the bar graphs. Data are mean±SEM of 4 to 14 experiments. \* and † indicate significant difference in corresponding response in endothelium-intact arteries with respect to BMS-191095 and diazoxide respectively (*P*<0.05).

reduced the vasodilation to 50  $\mu\text{mol/L}$  BMS (25.6 $\pm$ 2.4%,  $n=5$ ;  $P<0.05$ ) and 50  $\mu\text{mol/L}$  diazoxide (10.6 $\pm$ 1.4%,  $n=5$ ;  $P<0.05$ ), implicating PI3K in the vasodilation. Finally, inhibition of NOS with L-NAME resulted in diminished vasodilation to 50  $\mu\text{mol/L}$  BMS (25.6 $\pm$ 4%,  $n=8$ ;  $P<0.05$ ) and 50  $\mu\text{mol/L}$  diazoxide (10.4 $\pm$ 1.2%,  $n=6$ ;  $P<0.05$ ), suggesting that the major part of the vasodilation to BMS and diazoxide was mediated by NO (Figure 2A and 2B).

Arteries took  $\approx$ 20 to 30 minutes to attain a stable diameter both before and after the administration of pharmacological agents. In general, addition of pharmacological blockers had minimal effects on the diameter of precontracted arteries. When compared with vehicle-treated arteries (0.5 $\pm$ 0.4%,  $n=27$ ), pretreatment with L-NAME (8.9 $\pm$ 1.2%,

$n=14$ ;  $P<0.05$ ) caused slight constriction of arteries, whereas pretreatment with wortmannin (8.2 $\pm$ 5%,  $n=5$ ;  $P<0.05$ ) caused only slight vasodilation. However, pretreatment with MnTBAP (0.45 $\pm$ 0.7%,  $n=10$ ), 5-hydroxydecanoic acid (0.6 $\pm$ 1%,  $n=14$ ), fluoxetine (-0.7 $\pm$ 4%,  $n=5$ ), and glibenclamide (-0.1 $\pm$ 1%,  $n=6$ ) had no significant effect on vascular diameter.

### Mitochondrial Membrane Potential, [Ca<sup>2+</sup>]<sub>i</sub>, NO, and Mitochondrial ROS Measurements

The BMS and diazoxide depolarized the mitochondria of CMVECs indicated by reduction of rhodamine 123 fluorescence compared with vehicle-treated cells (Figure 3A and 3E). Background subtracted rhodamine 123 fluorescence

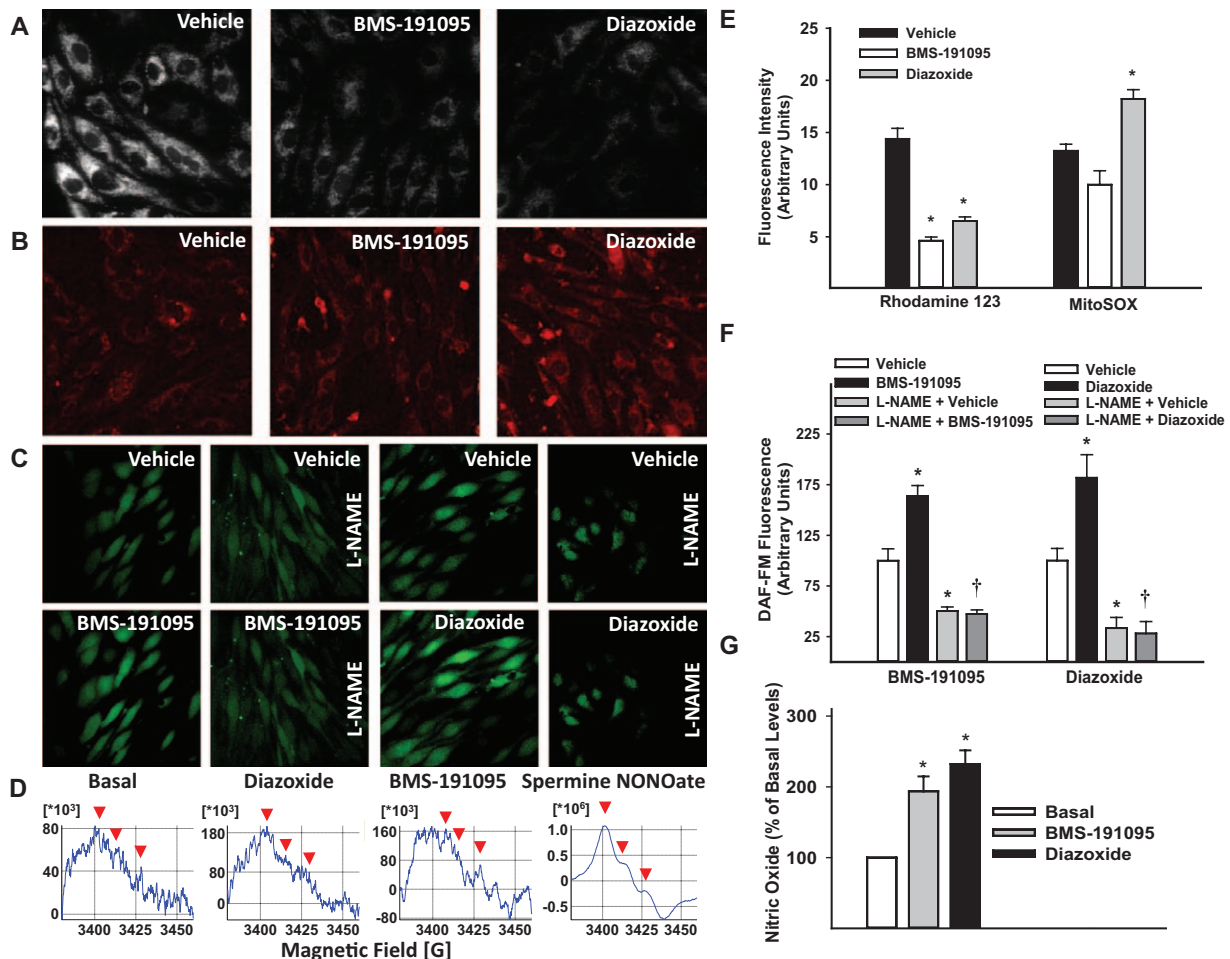


**Figure 3.** Fluorescence images of cultured primary rat brain microvascular endothelial cells (CMVECs) loaded with various fluorescent probes treated with vehicle (DMSO) or 50  $\mu\text{mol/L}$  BMS-191095 (BMS) or 100  $\mu\text{mol/L}$  diazoxide are shown. Fluorescence images of CMVECs loaded with rhodamine 123, a mitochondrial membrane potential marker, are shown in **A**. Mitochondrial depolarization is marked by the decrease in fluorescence. Fluorescence images of MitoSOX, a mitochondrial ROS-sensitive dye, are shown in **B**. **C**, Images of CMVECs loaded with 4-amino-5-methylamino-2',7'-difluorofluorescein diacetate (DAF-FM), a nitric oxide (NO)-sensitive dye, and treated with or without N<sup>o</sup>-nitro L-arginine methyl ester (L-NAME). Electron spin resonance (ESR) spectra of rat aortas incubated for 90 minutes at 37°C with 0.4 mmol/L colloid iron diethyldithiocarbamate, Fe<sup>2+</sup>(DETC)<sub>2</sub>, are shown in **D**. The vertical axis represents signal intensity in arbitrary units, and the horizontal axis represents the magnetic field (**G**). A characteristic NO-Fe(DETC)<sub>2</sub> signal with 3 peaks (indicated by **arrows**) was detected in rat aortas incubated with Fe(DETC)<sub>2</sub> and various drugs. The representative ESR spectra of the basal (vehicle-treated), 100  $\mu\text{mol/L}$  diazoxide, 50  $\mu\text{mol/L}$  BMS, and 10  $\mu\text{mol/L}$  spermine NONOate (10  $\mu\text{mol/L}$ , N-[2-Aminoethyl]-N-[2-hydroxy-2-nitrosohydrazino]-1,2-ethylenediamine)-treated aortas are shown along with the cumulative data expressed as percentage change from basal level as a bar graph (**G**). The cumulative data of fluorescence intensity from the images were determined and plotted as a bar graph for rhodamine 123, MitoSOX, and DAF-FM (**E** and **F**). In **E**, \*significant difference in response vs vehicle for corresponding fluorescent probes ( $P<0.05$ ). In **F**, \* and † indicate significant difference in response vs vehicle and untreated BMS or diazoxide, respectively ( $P<0.05$ ). In **G**, \* indicates significant difference in response vs basal level of normalized NO-Fe(DETC)<sub>2</sub> signal ( $P<0.05$ ).



(arbitrary units) was reduced to  $4.6 \pm 0.3$  by BMS ( $n=6$ ) and  $6.5 \pm 0.4$  by diazoxide ( $n=8$ ) treatment versus  $14.4 \pm 1$ , in vehicle-treated ( $n=6$ ) cells. Measurements of MitoSOX fluorescence (arbitrary units) showed that BMS-treated CMVECs did not display increased fluorescence ( $10 \pm 1.3$ ,  $n=5$ ;  $P=NS$ ) compared with the vehicle ( $13.3 \pm 0.6$ ,  $n=8$ ), indicating ROS production from mitochondria was unchanged (Figure 3B and 3E). In contrast, diazoxide treatment enhanced the fluorescence ( $18.2 \pm 0.9$ ,  $n=7$ ;  $P<0.05$ ) compared with vehicle-treated cells, indicating generation of ROS (Figure 3B and 3E). In addition, normalized measurements of DAF-FM in CMVECs showed increased fluorescence intensity in response to BMS ( $164 \pm 10\%$ ,  $n=7$ ;  $P<0.05$ ) and diazoxide ( $182 \pm 23\%$ ,  $n=6$ ;  $P<0.05$ ) compared with the vehicle ( $100 \pm 11\%$  and  $100.1 \pm 12\%$ , respectively;  $n=6$  each), indicating generation of NO. Inhibition of NOS with L-NAME pretreatment of CMVECs abolished enhanced DAF fluorescence in response to BMS ( $47.3 \pm 4\%$ ,  $n=7$ ;  $P<0.05$ ) and diazoxide ( $28.2 \pm 12\%$ ,  $n=6$ ;  $P<0.05$ ) compared with response in untreated CMVECs. L-NAME pretreatment reduced the DAF-FM fluorescence in vehicle-administered cells ( $50.3 \pm 4\%$  and  $33.3 \pm 11\%$ , controls of BMS and diazoxide, respectively;  $n=6$  each), however, this was a result of reduction in basal NO production that was sensitive to L-NAME. Thus, the increase in DAF fluorescence in response to BMS and diazoxide correlated with NOS-derived NO production (Figure 3C and 3F). Measurements of fluo-4 acetoxymethyl ester (fluo-4 AM)-loaded endothelial cells in freshly isolated cerebral arteries (Figure 4A and 4C) showed increase in fluorescence in response to BMS ( $172 \pm 20\%$ ,  $n=7$ ;  $P<0.05$ ) and diazoxide ( $185 \pm 23\%$ ,  $n=5$ ;  $P<0.05$ ) compared with vehicle ( $100 \pm 15\%$ ,  $n=6$ ). Similarly, fluo-4 AM-loaded CMVECs (Figure 4B and 4C) showed increase in fluorescence in response to BMS ( $23.6 \pm 3\%$ ,  $n=6$ ;  $P<0.05$ ) and diazoxide ( $25.7 \pm 3\%$ ,  $n=6$ ;  $P<0.05$ ) compared with vehicle ( $14.5 \pm 2\%$ ,  $n=6$ ). In addition, treatment of CMVECs with  $100 \mu\text{mol/L}$  BMS increased fluo-4 AM fluorescence ( $196 \pm 14\%$ ,  $n=4$ ;  $P<0.05$ ), but did not affect MitoSOX ( $100 \pm 7\%$ ,  $n=4$ ;  $P=NS$ ) fluorescence compared with vehicle-treated cells ( $145 \pm 8\%$ ,  $n=4$  and  $102 \pm 5\%$ ,  $n=4$ ; respectively; Figure II in the online-only Data Supplement). Thus, endothelial cells exhibited an increase in fluo-4 AM fluorescence in response to BMS and diazoxide, indicating elevation of cytosolic  $[\text{Ca}^{2+}]_i$  in the cells.

### NO Measurements by ESR

A characteristic NO-Fe(DETC)<sub>2</sub> signal with 3 peaks ( $g$  value  $\approx 2.035$ ) was detected in rat aortas incubated with Fe(DETC)<sub>2</sub> and various drugs. The magnitude of this signal was greatly increased by stimulation with the BMS ( $194 \pm 21\%$ ,  $n=6$ ;  $P<0.05$ ) or diazoxide ( $232 \pm 19\%$ ,  $n=6$ ;  $P<0.05$ ) compared with vehicle-treated aortas ( $100 \pm 0\%$ ,  $n=6$ ; Figure 3D and 3G). Furthermore, the ESR signals from BMS- or diazoxide-stimulated aortas were abolished after addition of the NOS inhibitor, L-NAME.

### Akt and eNOS Phosphorylation

Treatment of CMVECs with BMS ( $2.08 \pm 0.21$ ,  $n=8$ ;  $P<0.05$ ) and diazoxide ( $1.83 \pm 0.17$ ,  $n=8$ ;  $P<0.05$ ) led to increased phosphorylated-Akt/total-Akt ratio of immunoband intensity (arbitrary units), compared with vehicle treatment ( $1.12 \pm 0.13$ ,  $n=8$ ; Figure 5A and 5C). Similarly, treatment of arteries with BMS ( $1.31 \pm 0.03$ ,  $n=5$ ;  $P<0.05$ ) and diazoxide ( $1.24 \pm 0.05$ ,  $n=5$ ;  $P<0.05$ ) promoted increased phosphorylated-Akt/total-Akt ratio of immunoband intensity compared with vehicle-treated arteries ( $0.84 \pm 0.03$ ,  $n=5$ ; Figure 5A and 5C). Treatment of CMVECs with BMS ( $1.29 \pm 0.059$ ,  $n=8$ ;  $P<0.05$ ) and diazoxide ( $1.29 \pm 0.06$ ,  $n=8$ ;  $P<0.05$ ) led to increased phosphorylated-eNOS/total-eNOS ratio of immunoband intensity compared with vehicle-treated arteries ( $1.0 \pm 0.028$ ,  $n=8$ ; Figure 5A and 5D). Similarly, treatment of arteries with BMS ( $0.82 \pm 0.03$ ,  $n=5$ ;  $P<0.05$ ) and diazoxide ( $1.01 \pm 0.06$ ,  $n=5$ ;  $P<0.05$ ) induced increased phosphorylated-eNOS/total-eNOS ratio of immunoband intensity compared with vehicle-treated arteries ( $0.72 \pm 0.03$ ,  $n=5$ ; Figure 5A and 5D). In addition, the phosphorylated-eNOS/total-eNOS

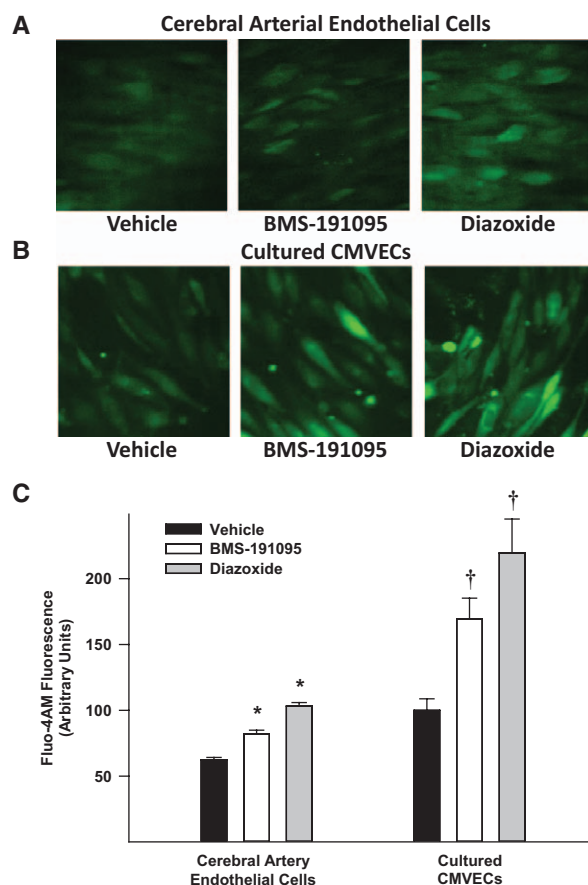


**Figure 4.** Fluorescence images of cerebral artery endothelial cells (A) and cultured primary rat brain microvascular endothelial cells (CMVECs; B) loaded with fluo-4 AM, a calcium-sensitive fluoroprobe, and treated with vehicle (DMSO) or  $50 \mu\text{mol/L}$  BMS-191095 (BMS). The cumulative data of fluorescence intensity from the images were determined and plotted as a bar graph in C. \* and † indicate significant difference in response to BMS or diazoxide vs vehicle, in arterial endothelial cells or CMVECs, respectively ( $P<0.05$ ).

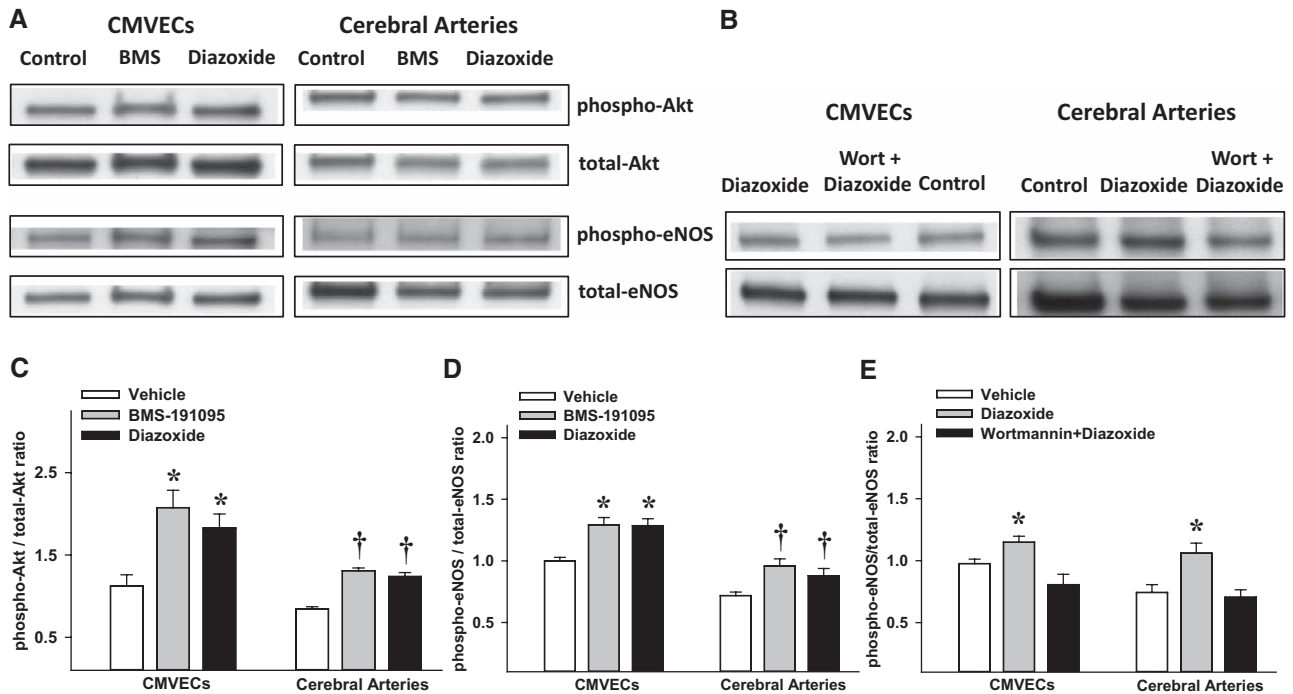


**Figure 5.** Western blots of total and phosphorylated forms of Akt and endothelial nitric oxide synthase (eNOS) in homogenates of cultured primary rat brain microvascular endothelial cells (CMVECs) and cerebral arteries treated with vehicle (control) or BMS-191095 (BMS) or diazoxide are shown (A). In B, Western blots of total and phosphorylated forms of eNOS in homogenates of CMVECs and cerebral arteries treated with vehicle or diazoxide or diazoxide+wortmannin are shown. The cumulative data (mean±SEM) from the immunoband intensities were expressed as ratio of phosphorylated Akt to total Akt (C), and phosphorylated eNOS to total eNOS (D and E). \* and † indicate significant difference compared with corresponding vehicle-treated CMVECs and arteries, respectively ( $P<0.05$ ). Wort indicates wortmannin.

ratio of immunoband intensities showed an increase in response to diazoxide ( $1.15\pm 0.05$ ,  $n=6$ ;  $P<0.05$ ) compared with vehicle-treated CMVECs ( $0.98\pm 0.04$ ,  $n=6$ ;  $P=NS$ ), and wortmannin pretreatment abolished the diazoxide response ( $0.81\pm 0.08$ ,  $n=6$ ;  $P<0.05$ ; Figure 5B and 5E). Similarly, in cerebral arteries, the phosphorylated-eNOS/total-eNOS ratio of immunoband intensities showed an increase in response to diazoxide ( $1.06\pm 0.08$ ,  $n=3$ ;  $P<0.05$ ) compared with vehicle-treated arteries ( $0.74\pm 0.06$ ,  $n=3$ ;  $P=NS$ ), and wortmannin pretreatment abolished diazoxide response ( $0.7\pm 0.06$ ,  $n=3$ ;  $P<0.05$ ; Figure 5B and 5E). Thus, pretreatment of CMVECs and arteries with wortmannin eliminated the increase in eNOS phosphorylation in response to diazoxide.

## Discussion

There are 4 major, new findings of the study. First, mitochondrial depolarization in the presence as well as in the absence of ROS generation is a potent initiator of dilator responses of cerebral arteries. Second, mitochondrial depolarization-induced relaxation involves contributions from endothelium as well as VSM. Third, the endothelium-dependent vasodilation induced by mitochondrial depolarization is mediated by NO resulting from activation of eNOS via increased endothelial  $[Ca^{2+}]_i$  and activation of PI3K leading to Akt phosphorylation. Fourth, both mitochondrial ROS-dependent and -independent mechanisms are capable of promoting vasodilation by mitochondrial depolarization. Our observations indicate that

mitochondrial factors specific to depolarization can have major influences on the regulation of cerebral vascular tone.

Our finding that activation of  $mitoK_{ATP}$  channels elicited vasodilation is consistent with previous studies from our laboratory<sup>3</sup> and others,<sup>2</sup> and in addition, demonstrates the importance of the endothelium. Scavenging of ROS reduced the vasodilation response to diazoxide alone, whereas BMS-induced vasodilation was unaffected. Thus, the ability of mitochondrial depolarization by BMS to promote vasodilation independent of ROS generation is a novel observation. Measurements of mitochondrial ROS in endothelial cells provided additional evidence that, unlike diazoxide, BMS does not enhance the generation of mitochondrial ROS. Furthermore, reduced vasodilation in response to BMS and diazoxide after endothelial denudation confirmed the important contribution of endothelium to mitochondria-mediated vasodilation. Notably, the greater endothelial contribution to vasodilation in response to BMS versus diazoxide suggests that the ROS production by diazoxide may interfere with NO-dependent mechanisms.

Mitochondria-mediated vasodilation was also sensitive to inhibition of  $mitoK_{ATP}$  channels confirming their role in mitochondrial depolarization. Studies in our laboratory and others have demonstrated the role of  $mitoK_{ATP}$  channels in mediating the effects of diazoxide<sup>2,14,22</sup> and BMS<sup>3,12,13,16,18,19,21,23,24</sup> in isolated mitochondria, neurons, vasculature, and cardiomyocytes. Also, our laboratory has characterized the distinct ROS-independent mechanism of actions of BMS compared

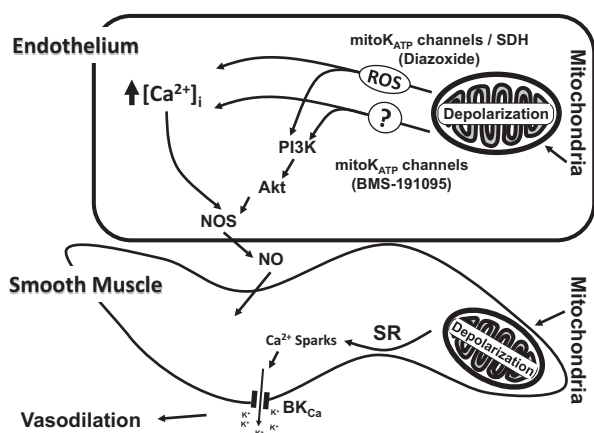


**Figure 6.** A schematic of the proposed mechanisms underlying the vasodilation induced by the mitochondrial depolarization in the endothelium. Depolarization of mitochondria leads to elevation of endothelial  $[Ca^{2+}]_i$  by both reactive oxygen species (ROS)-dependent and -independent mechanisms. Elevation of global endothelial  $[Ca^{2+}]_i$  promotes activation of endothelial nitric oxide synthase (eNOS), which, in turn, leads to generation of nitric oxide (NO). Mitochondrial depolarization in endothelial cells also promotes activation of phosphoinositide-3 kinase (PI3K), phosphorylation of Akt, and subsequently phosphorylation of eNOS resulting in  $[Ca^{2+}]_i$ -independent activation of eNOS leading to NO generation. Finally, mitochondrial depolarization-induced endothelium-dependent vasodilation is primarily mediated by NO, and this effect enhances vascular smooth muscle (VSM)-specific relaxation. Mitochondrial depolarization in VSM cells sequentially causes the activation of ryanodine-sensitive  $Ca^{2+}$  channels on sarcoplasmic reticulum, generation of calcium transients, calcium sparks, and the opening of adjacent large-conductance calcium-activated potassium channels ( $BK_{Ca}$ ) on the plasma membrane. The efflux of  $K^+$  thus leads to hyperpolarization, decreased global intracellular  $Ca^{2+}$  of smooth muscle, and vasodilation.

with diazoxide in isolated mitochondria and cultured cortical neurons.<sup>12,16</sup> The present study confirms our previous findings of ROS-independent actions of BMS in promoting mitochondria-mediated vasodilation.

Inhibition of NOS diminished vasodilation to BMS and diazoxide in endothelium-intact arteries indicating that part of the mitochondria-mediated vasodilation was NO-dependent vasodilation. This finding is consistent with our previous observations, which showed that diazoxide-induced vasodilation involved endothelium and NOS.<sup>3</sup> Moreover, fluorescence measurements of NO in CMVECs confirmed the ability of BMS and diazoxide to enhance NO generation sensitive to NOS inhibition. Furthermore, measurements of NO by ESR provided additional evidence supporting the ability of BMS and diazoxide to promote NO generation in vascular tissues. Two potential mechanisms underlie the activation of eNOS in response to BMS and diazoxide: First, fluorescence measurements of  $Ca^{2+}$  showed elevation of intracellular  $Ca^{2+}$  in response to mitochondrial depolarization in CMVECs and also in endothelial cells of intact cerebral arteries, thus implicating  $[Ca^{2+}]_i$  in the production and release of endothelial-relaxing factors. Second, administration of wortmannin resulted in diminished vasodilation in response to BMS and diazoxide, implicating the PI3K pathway in vasodilation. Mitochondrial depolarization initiates key elements of cellular signaling, such as activation of Akt or

increases in  $[Ca^{2+}]_i$ , events which are associated with direct effects on VSM and production of endothelium-dependent relaxing factors, such as NO and prostacyclin.<sup>3</sup> For example, we have recently shown that insulin dilates cerebral arteries after activation of the PI3K and Akt system.<sup>25</sup> Our findings showing that wortmannin reduced vasodilation to BMS and diazoxide are consistent with this mechanism, and similar findings have been reported in heart.<sup>21</sup> In addition, BMS and diazoxide treatment of CMVECs and arteries promoted phosphorylation of Akt consistent with involvement of PI3K–Akt pathway in vasodilation.<sup>26</sup> Our previous studies reported for the first time that mitochondrial depolarization leads to the activation of PI3K–Akt signaling pathway in cultured neurons,<sup>12</sup> as opposed to PI3K–Akt pathway activation leading to alteration of mitochondrial membrane potential.<sup>27</sup> Mitochondrial depolarization has been shown to increase localized calcium transients in the form of  $Ca^{2+}$  sparks in VSM<sup>2</sup> without significant change in global  $[Ca^{2+}]_i$ , however, the exact mechanisms by which mitochondrial depolarization leads to an increase in  $[Ca^{2+}]_i$ , and activation of PI3K in endothelial cells needs further investigation. We believe that the mechanisms underlying the release of NO are likely to promote the release of non-NO factors, such as hydrogen peroxide, prostacyclin, and so on, contributing to mitochondria-mediated vasodilation. Furthermore, treatment of cerebral arteries and CMVECs with BMS and diazoxide resulted in increased phosphorylation of eNOS, further confirming the activation of eNOS by mitochondrial depolarization. Finally, wortmannin abolished the diazoxide-induced increase in phosphorylation of eNOS in both CMVECs and arteries confirming the role of the PI3K pathway in mitochondria-mediated vasodilation.

Although this is a relatively new field of study, it appears that diverse physiological, pathological, and pharmacological factors can depolarize mitochondria in vascular cells. Depolarization of mitochondria in other nonvascular cells within the neurovascular unit, such as astroglia and neurons, might also lead to the production and release of substances, which could affect cerebral vascular tone. Thus, increased shear stress in coronary arteries, possibly through filamentous connections with the glycocalyx, can distort and activate mitochondrial-driven events resulting in production of dilator agents, such as hydrogen peroxide in mitochondria.<sup>28</sup> Similarly, decreased oxygen levels can affect mitochondrial membrane potential in blood vessels.<sup>2,10</sup> Furthermore, we have shown that drugs such as rosuvastatin also depolarize mitochondria in neurons.<sup>29</sup> Thus, our findings have demonstrated for the first time the ability of mitochondrial depolarization to promote the release of endothelial-relaxing factors via increased  $[Ca^{2+}]_i$  and the PI3K–Akt–eNOS pathway.

### Limitations

Our studies used pharmacological approaches to promote mitochondrial depolarization, and agents such as diazoxide have been shown to exhibit some nontarget and nonspecific mitochondrial effects. Many physiological/pathological stimuli (hypoxia)<sup>30,31</sup> that promote mitochondrial depolarization are plagued by similar, but significantly greater



nonspecific effects. Importantly, diazoxide is a widely used well-characterized mitochondrial agent. We and others have studied diazoxide and BMS in variety of cell types. Despite recent evidence,<sup>32</sup> there is a lack of consensus on the molecular identity of the mitoK<sub>ATP</sub> channel, specificity of its blockers, and their role in mitochondrial depolarization. Our purpose of using pharmacological agents was to achieve mitochondrial depolarization with minimal nontarget effects. The primary mechanisms of elevation of endothelial global [Ca<sup>2+</sup>]<sub>i</sub>, phosphorylation of Akt, and eNOS in response to diazoxide and BMS were qualitatively similar, implicating mitochondrial depolarization as the common activator of these pathways.

In summary, our study has uncovered a novel mitochondria-mediated mechanism of vasodilation in cerebral arteries, which involves the release of endothelium-derived relaxing factors in response to mitochondrial depolarization. Activation of ROS-dependent and ROS-independent signaling pathways after mitochondrial depolarization leads to complex cellular events involving release of endothelial factors, which lead to a vascular response to match cerebral blood flow with metabolism.

### Acknowledgments

We thank Nancy Busija, MA, SLP, for the help with editing the manuscript. In addition, we thank Dan Liu for technical assistance with Western blot experiments.

### Sources of Funding

This work was supported by the National Institutes of Health grant numbers HL-077731, HL-030260, HL093554, and HL-065380 (D.W.B.), and the Ja'nos Bolyai Research Scholarship of the Hungarian Academy of Sciences and National Scientific Research Fund of Hungary grant number OTKA K68976 (F.D.).

### Disclosures

None.

### References

- Cheranov SY, Jaggar JH. Mitochondrial modulation of Ca<sup>2+</sup> sparks and transient K<sub>Ca</sub> currents in smooth muscle cells of rat cerebral arteries. *J Physiol (Lond)*. 2004;556:755–771.
- Xi Q, Cheranov SY, Jaggar JH. Mitochondria-derived reactive oxygen species dilate cerebral arteries by activating Ca<sup>2+</sup> sparks. *Circ Res*. 2005;97:354–362.
- Katakam PV, Domoki F, Snipes JA, Busija AR, Jarajapu YP, Busija DW. Impaired mitochondria-dependent vasodilation in cerebral arteries of Zucker obese rats with insulin resistance. *Am J Physiol Regul Integr Comp Physiol*. 2009;296:R289–R298.
- Zhang DX, Gutterman DD. Mitochondrial reactive oxygen species-mediated signaling in endothelial cells. *Am J Physiol Heart Circ Physiol*. 2007;292:H2023–H2031.
- Davidson SM, Duchon MR. Endothelial mitochondria: contributing to vascular function and disease. *Circ Res*. 2007;100:1128–1141.
- Liu Y, Zhao H, Li H, Kalyanaraman B, Nicolosi AC, Gutterman DD. Mitochondrial sources of H<sub>2</sub>O<sub>2</sub> generation play a key role in flow-mediated dilation in human coronary resistance arteries. *Circ Res*. 2003;93:573–580.
- Spitaler MM, Graier WF. Vascular targets of redox signalling in diabetes mellitus. *Diabetologia*. 2002;45:476–494.
- Ungvari Z, Labinskyy N, Mukhopadhyay P, Pinto JT, Bagi Z, Ballabh P, Zhang C, Pacher P, Csizsar A. Resveratrol attenuates mitochondrial oxidative stress in coronary arterial endothelial cells. *Am J Physiol Heart Circ Physiol*. 2009;297:H1876–H1881.
- Waypa GB, Guzy R, Mungai PT, Mack MM, Marks JD, Roe MW, Schumacker PT. Increases in mitochondrial reactive oxygen species trigger hypoxia-induced calcium responses in pulmonary artery smooth muscle cells. *Circ Res*. 2006;99:970–978.
- Weissmann N, Schermuly RT, Ghofrani HA, Hänze J, Goyal P, Grimminger F, Seeger W. Hypoxic pulmonary vasoconstriction—triggered by an increase in reactive oxygen species? *Novartis Found Symp*. 2006;272:196–208; discussion 208.
- Widlansky ME, Gutterman DD. Regulation of endothelial function by mitochondrial reactive oxygen species. *Antioxid Redox Signal*. 2011;15:1517–1530.
- Gáspár T, Snipes JA, Busija AR, Kis B, Domoki F, Bari F, Busija DW. ROS-independent preconditioning in neurons via activation of mitoK(ATP) channels by BMS-191095. *J Cereb Blood Flow Metab*. 2008;28:1090–1103.
- Kis B, Nagy K, Snipes JA, Rajapakse NC, Horiguchi T, Grover GJ, Busija DW. The mitochondrial K(ATP) channel opener BMS-191095 induces neuronal preconditioning. *Neuroreport*. 2004;15:345–349.
- Kis B, Rajapakse NC, Snipes JA, Nagy K, Horiguchi T, Busija DW. Diazoxide induces delayed pre-conditioning in cultured rat cortical neurons. *J Neurochem*. 2003;87:969–980.
- Rajapakse N, Kis B, Horiguchi T, Snipes J, Busija D. Diazoxide pretreatment induces delayed preconditioning in astrocytes against oxygen glucose deprivation and hydrogen peroxide-induced toxicity. *J Neurosci Res*. 2003;73:206–214.
- Busija DW, Katakam P, Rajapakse NC, Kis B, Grover G, Domoki F, Bari F. Effects of ATP-sensitive potassium channel activators diazoxide and BMS-191095 on membrane potential and reactive oxygen species production in isolated piglet mitochondria. *Brain Res Bull*. 2005;66:85–90.
- Schäfer G, Portenhauser R, Trolp R. Inhibition of mitochondrial metabolism by the diabetogenic thiazidine diazoxide. I. Action on succinate dehydrogenase and TCA-cycle oxidations. *Biochem Pharmacol*. 1971;20:1271–1280.
- Grover GJ, D'Alonzo AJ, Darbenzio RB, Parham CS, Hess TA, Bathala MS. In vivo characterization of the mitochondrial selective K(ATP) opener (3R)-trans-4-((4-chlorophenyl)-N-(1H-imidazol-2-ylmethyl)dimethyl-2H-1-benzopyran-6-carbonitril monohydrochloride (BMS-191095): cardioprotective, hemodynamic, and electrophysiological effects. *J Pharmacol Exp Ther*. 2002;303:132–140.
- Grover GJ, D'Alonzo AJ, Garlid KD, Bajgar R, Lodge NJ, Sleph PG, Darbenzio RB, Hess TA, Smith MA, Pauczek P, Atwal KS. Pharmacologic characterization of BMS-191095, a mitochondrial K(ATP) opener with no peripheral vasodilator or cardiac action potential shortening activity. *J Pharmacol Exp Ther*. 2001;297:1184–1192.
- Wang Y, Ahmad N, Wang B, Ashraf M. Chronic preconditioning: a novel approach for cardiac protection. *Am J Physiol Heart Circ Physiol*. 2007;292:H2300–H2305.
- Ahmad N, Wang Y, Haider KH, Wang B, Pasha Z, Uzun O, Ashraf M. Cardiac protection by mitoKATP channels is dependent on Akt translocation from cytosol to mitochondria during late preconditioning. *Am J Physiol Heart Circ Physiol*. 2006;290:H2402–H2408.
- Rajapakse N, Shimizu K, Kis B, Snipes J, Lacza Z, Busija D. Activation of mitochondrial ATP-sensitive potassium channels prevents neuronal cell death after ischemia in neonatal rats. *Neurosci Lett*. 2002;327:208–212.
- Neckár J, Szárszói O, Kóten L, Papoušek F, Ost'ádal B, Grover GJ, Kolár F. Effects of mitochondrial K(ATP) modulators on cardioprotection induced by chronic high altitude hypoxia in rats. *Cardiovasc Res*. 2002;55:567–575.
- Mayanagi K, Gáspár T, Katakam PV, Kis B, Busija DW. The mitochondrial K(ATP) channel opener BMS-191095 reduces neuronal damage after transient focal cerebral ischemia in rats. *J Cereb Blood Flow Metab*. 2007;27:348–355.
- Katakam PV, Domoki F, Lenti L, Gáspár T, Institoris A, Snipes JA, Busija DW. Cerebrovascular responses to insulin in rats. *J Cereb Blood Flow Metab*. 2009;29:1955–1967.
- Minshall RD, Sessa WC, Stan RV, Anderson RG, Malik AB. Caveolin regulation of endothelial function. *Am J Physiol Lung Cell Mol Physiol*. 2003;285:L1179–L1183.
- Wang S, Wang Y, Jiang J, Wang R, Li L, Qiu Z, Wu H, Zhu D. 15-HETE protects rat pulmonary arterial smooth muscle cells from apoptosis via the PI3K/Akt pathway. *Prostaglandins Other Lipid Mediat*. 2010;91:51–60.
- Liu Y, Li H, Bubolz AH, Zhang DX, Gutterman DD. Endothelial cytoskeletal elements are critical for flow-mediated dilation in human coronary arterioles. *Med Biol Eng Comput*. 2008;46:469–478.



29. Domoki F, Kis B, Gáspár T, Snipes JA, Parks JS, Bari F, Busija DW. Rosuvastatin induces delayed preconditioning against oxygen-glucose deprivation in cultured cortical neurons. *Am J Physiol, Cell Physiol.* 2009;296:C97–105.
30. Shimoda LA, Undem C. Interactions between calcium and reactive oxygen species in pulmonary arterial smooth muscle responses to hypoxia. *Respir Physiol Neurobiol.* 2010;174:221–229.
31. Gupte SA, Wolin MS. Oxidant and redox signaling in vascular oxygen sensing: implications for systemic and pulmonary hypertension. *Antioxid Redox Signal.* 2008;10:1137–1152.
32. Foster DB, Ho AS, Rucker J, Garlid AO, Chen L, Sidor A, Garlid KD, O'Rourke B. Mitochondrial ROMK channel is a molecular component of mitoK(ATP). *Circ Res.* 2012;111:446–454.

### Significance

Mitochondria play an important role in the regulation of vascular tone. Recent, limited evidence shows that mitochondrial depolarization promotes relaxation of intact or endothelium-denuded arteries or isolated vascular smooth muscle cells. Mitochondrial depolarization occurs in physiological (metabolic demand) and pathological (hypoxia-ischemia) conditions. However, the exact mechanisms by which mitochondrial depolarization promotes the release of endothelial vasoactive factors have not been adequately studied. In the present study, we induced endothelial mitochondrial depolarization by 2 mechanistically different selective activators of mitochondrial ATP sensitive potassium channels. We demonstrated that mitochondrial depolarization results in activation of endothelial NO synthase by dual pathways, involving increased intracellular calcium as well as by phosphoinositide-3 kinase-protein kinase B-induced endothelial NO synthase phosphorylation. Both mitochondrial reactive oxygen species-dependent and –independent mechanisms mediate activation of endothelial NO synthase by endothelial mitochondrial depolarization. Thus, present study provides the first evidence of the mechanism by which mitochondria may match metabolic demand with blood flow.

## SUPPLEMENT MATERIAL

### Depolarization of Mitochondria in Endothelial Cells Promotes Cerebral Vascular Vasodilation by Activation of Nitric Oxide Synthase

Prasad V.G. Katakam,<sup>1,2</sup> Edina Wappler,<sup>1,2</sup> Paige Katz,<sup>1</sup> Ibolya Rutkai,<sup>1</sup> Adam Institoris,<sup>2,3</sup>  
Ferenc Domoki,<sup>2,3</sup> Tamás Gáspár,<sup>2</sup> Samuel Grovenberg,<sup>1</sup> James A. Snipes,<sup>2</sup> and David W.  
Busija<sup>1,2</sup>.

<sup>1</sup>Department of Pharmacology, Tulane University School of Medicine, New Orleans, Louisiana;

<sup>2</sup>Department of Physiology and Pharmacology, Wake Forest University Health Sciences,  
Winston Salem, North Carolina; <sup>3</sup>Department of Physiology, University of Szeged Medical  
School, Szeged, Hungary.

**Corresponding Author:** Prasad V.G. Katakam, M.D., Ph.D.

1430 Tulane Avenue, New Orleans, Louisiana 70112

Phone: 504-988-1426

Fax: 504-988-5283

Email: [pkatakam@tulane.edu](mailto:pkatakam@tulane.edu)

## MATERIALS AND METHODS

### Fluorescence Confocal Microscopy.

1. Mitochondrial membrane potential was determined by using rhodamine 123, ( $\lambda_{\text{ex}}$ : 488 nm,  $\lambda_{\text{em}}$ : >505 nm long pass filter). 2. MitoSOX ( $\lambda_{\text{ex}}$ : 405 nm,  $\lambda_{\text{em}}$ : >560 nm long pass filter) was used to measure mitochondrial ROS, specifically superoxide, based on the method reported by Robinson et al <sup>1</sup>. Several previous studies measured the MitoSOX fluorescence with  $\lambda_{\text{ex}}$ : 488 nm,  $\lambda_{\text{em}}$ : >560 nm. However, recent studies by Robinson et al <sup>1</sup> provided evidence that MitoSOX fluorescence, when the fluoroprobe is excited at a wave length of  $\lambda_{\text{ex}}$ : 405 nm and emission is captured at a wavelgth of  $\lambda_{\text{em}}$ : >560 nm, is specific for measurement of superoxide. 3. Fluo-4 AM ( $\lambda_{\text{ex}}$ : 488 nm,  $\lambda_{\text{em}}$ : 505 nm long pass filter) was used to study  $[\text{Ca}^{2+}]_i$ . 4. 4-amino-5-methylamino- 2',7'-difluorofluorescein diacetate (DAF-FM,  $\lambda_{\text{ex}}$ : 488 nm,  $\lambda_{\text{em}}$ : >505 nm long pass filter) was used to measure NO. The specificity of NO measurements was established by inhibition of NO generation by NOS with L-NAME.

Stock solutions of fluoroprobes were prepared in DMSO. The CMVECs were loaded in the dark with a 1:1 mixture of 5 $\mu\text{mol/L}$  fluo-4 AM or 5 $\mu\text{mol/L}$  DAF-FM and 20% (w/v) pluronic F-127 diluted in PBS containing glucose (1g/L) for 30 min at room temperature. For  $[\text{Ca}^{2+}]_i$  measurements in arterial endothelial cells, freshly isolated rat posterior cerebral arteries were cut longitudinally, and pinned to a Sylgard block with the endothelium facing up as previously described. <sup>2</sup> Subsequently, fluo-4 AM was loaded, as described above, with the arterial segment pinned to the sylgard block, mounted in a vessel chamber with the endothelium facing the cover slip, and the objective on the inverted microscope. Cells were washed and incubated for a further 30 min to allow for complete de-esterification of intracellular AM esters and diacetates. Rhodamine 123 (5  $\mu\text{g/ml}$ ) or MitoSOX ( 5 $\mu\text{mol/L}$ ) solutions were prepared in phenol-free



DMEM and CMVECs were loaded with fluoroprobes for 15 min at 37°C. Confocal microscopy was performed using a laser scanning confocal system (LSM 510 and 7 Live; Zeiss, Jena, Germany) attached to an inverted microscope with a Zeiss C-Apochromat 63X /NA 1.2 water immersion objective. MitoSOX fluorescence was determined by Leica SP2 AOB laser confocal microscope. Fluorescence images were acquired before and after application of vehicle (dimethyl sulfoxide, DMSO) or BMS (50 µmol/L or 100 µmol/L) or diazoxide (100 µmol/L ) for rhodamine 123, fluo-4 AM, and MitoSOX whereas DAF-FM images were acquired with or without a 30 min L-NAME pretreatment of cells. Imaging conditions such as gain levels and laser power were held constant. Offline analysis of images to determine the average pixel intensity of endothelial cells in each field ( $n=20-30$ ) was performed using ImageJ software (National Institute of Health, Bethesda, MD) and the results were expressed in relative fluorescence units (RFUs) expressed as % change from the baseline images prior to administration of vehicle or BMS or diazoxide. For each coverslip with cells, 10-15 randomly selected fields containing 15-20 cells were imaged following vehicle or BMS or diazoxide treatment. Average fluorescence intensity of all the cells in the image was determined first followed by determination of the average of all images acquired from each cover slip. The 'n' value represents average fluorescence intensity of all the cells from 'n' number of cover slips that were included with each treatment.

### **NO Measurements**

The NO measurements were performed using electron spin resonance (ESR) spectroscopy using the previously published methods<sup>3,4</sup>

**Colloid Fe(DETC)<sub>2</sub> spin trapping.** DETC (7.2 mg/10ml) and FeSO<sub>4</sub> 7H<sub>2</sub>O (4.5mg/10ml) were separately dissolved under argon gas bubbling in two 10ml volumes of ice-

cold modified Krebs–Hepes buffer (K-H) containing (in mmol/L) 99.01 NaCl, 4.69 KCl, 1.87 CaCl<sub>2</sub>, 1.20 MgSO<sub>4</sub>, 25 NaHCO<sub>3</sub>, 1.03 K<sub>2</sub>HPO<sub>4</sub>, 20 sodium-HEPES, and 11.1 d-glucose, pH 7.35. These were rapidly mixed to obtain a pale yellow-brown opalescent colloid Fe(DETC)<sub>2</sub> solution (0.4mmol/L) which was used immediately. Aortas were placed separately in 12-well plates, each filled with 1 ml K-H buffer, in the presence and absence vehicle (DMSO), BMS (50 μmol/L), diazoxide (100 μmol/L), or spermine NONOate [10 μmol/L, N-(2-Aminoethyl)-N-(2-hydroxy-2-nitrosohydrazino)-1,2-ethylenediamine] to stimulate NOS. Colloid Fe(DETC)<sub>2</sub> was then added to each well (0.4 mmol/L) and incubated at 37 °C for 90 min. Separate experiments were completed to examine the effects of NOS inhibition by addition of NG-nitro-L-arginine methyl ester (L-NAME) to the incubation medium (final concentration 1mM). Incubations were also performed with colloid Fe(DETC)<sub>2</sub> alone (without aortas) to correct for any background signals.

**ESR spectroscopy.** After incubation, the aortic segments were removed and frozen in liquid nitrogen, and placed in the middle of a column of K-H buffer as follow: The needle-end was cut from a 1 ml syringe barrel, the plunger retracted 1.5 cm from the cut end, and aortic segments were placed into the syringe barrel, which was then filled with K-H buffer and frozen in liquid nitrogen. After freezing, the syringe was removed from the liquid nitrogen and warmed for 5 s; the plunger was then removed, and the remaining barrel was filled with K-H buffer and frozen in liquid nitrogen. The syringe was then re-warmed for 5 s, and the syringe plunger was used to push the frozen column out of the syringe barrel directly into a finger dewar (Noxygen Science Transfer & Diagnostics GmbH, Elzach, Germany) containing liquid nitrogen. The ESR spectra were obtained using a benchtop X-band EMX series ESR spectrometer (Bruker Biospin GmbH, Karlsruhe, Germany) using a high sensitivity SHQ microwave cavity in a finger dewar

filled with liquid nitrogen. The ESR spectrometer settings were as follows: microwave power 40 mW, modulation amplitude 8 G center-field 2.03 g, sweep width 80 G, conversion time 80 msec, time constant 20 msec, sweep time 10.24 s, with 60 scans. Signals were quantified by measuring the total amplitude after correction of baseline. The amount of NO was determined by measuring the total amplitude of the ESR signal for each treatment and comparing it with the ESR signal amplitude of the signal following NO-donor spermine NONOate. Finally, diazoxide and BMS induced NO production in aortas are expressed as % change from basal levels (vehicle treated).

A characteristic NO-Fe(DETC)<sub>2</sub> signal with three peaks (g value approximately 2.035) was detected in rat aortas incubated with Fe(DETC)<sub>2</sub> and various drugs. The amount of NO was determined by measuring the total amplitude of the ESR signal for each treatment and comparing with the ESR signal amplitude of the signal following NO-donor spermine NONOate. Finally, diazoxide and BMS induced NO production in aortas are expressed as % change from basal levels (vehicle treated) (Figure II). Furthermore, the ESR signals from BMS or diazoxide-stimulated aortas were abolished after addition of the NOS inhibitor, L-NAME.

## REFERENCES

1. Robinson KM, Janes MS, Beckman JS. The selective detection of mitochondrial superoxide by live cell imaging. *Nat Protoc.* 2008;3:941-947.
2. Ledoux J, Taylor MS, Bonev AD, Hannah RM, Solodushko V, Shui B, Tallini Y, Kotlikoff MI, Nelson MT. Functional architecture of inositol 1,4,5-trisphosphate signaling in restricted spaces of myoendothelial projections. *Proc Natl Acad Sci U S A.* 2008;105:9627-9632.
3. Cai H, Li Z, Dikalov S, Holland SM, Hwang J, Jo H, Dudley SC, Jr., Harrison DG. NAD(P)H oxidase-derived hydrogen peroxide mediates endothelial nitric oxide production in response to angiotensin II. *J Biol Chem.* 2002;277:48311-48317.
4. Fink B, Dikalov S, Fink N. ESR techniques for the detection of nitric oxide in vivo as an index of endothelial function. *Pharmacol Rep.* 2006;58 Suppl:8-15.



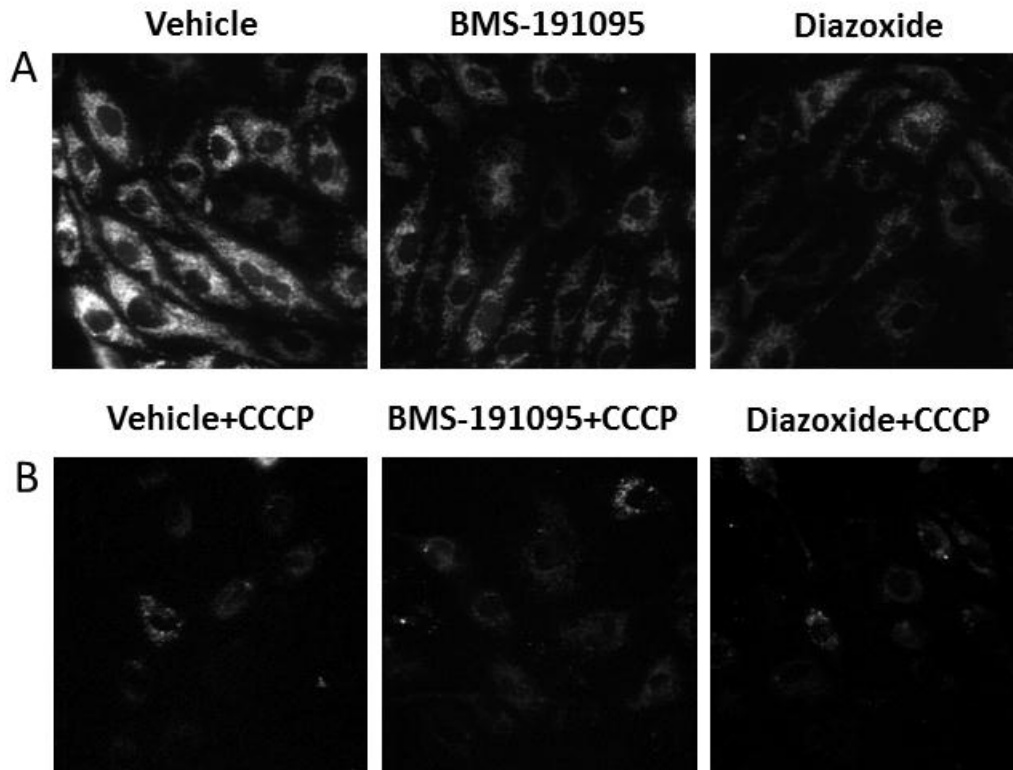


**Figure I.** Fluorescence images of CMVECs loaded with rhodamine 123, a mitochondrial membrane potential sensitive fluoroprobe and treated with vehicle (DMSO) or 50  $\mu\text{mol/L}$  BMS followed by depolarization with carbonyl cyanide 3-chlorophenylhydrazone (CCCP, a protonophore and uncoupler of oxidative phosphorylation in mitochondria). Treatment with 5  $\mu\text{mol/L}$  CCCP abolished the rhodamine 123 fluorescence confirming the localization of the fluoroprobe to mitochondria and also specificity of changes in the rhodamine 123 fluorescence to changes in mitochondrial membrane potential in response to BMS and diazoxide.

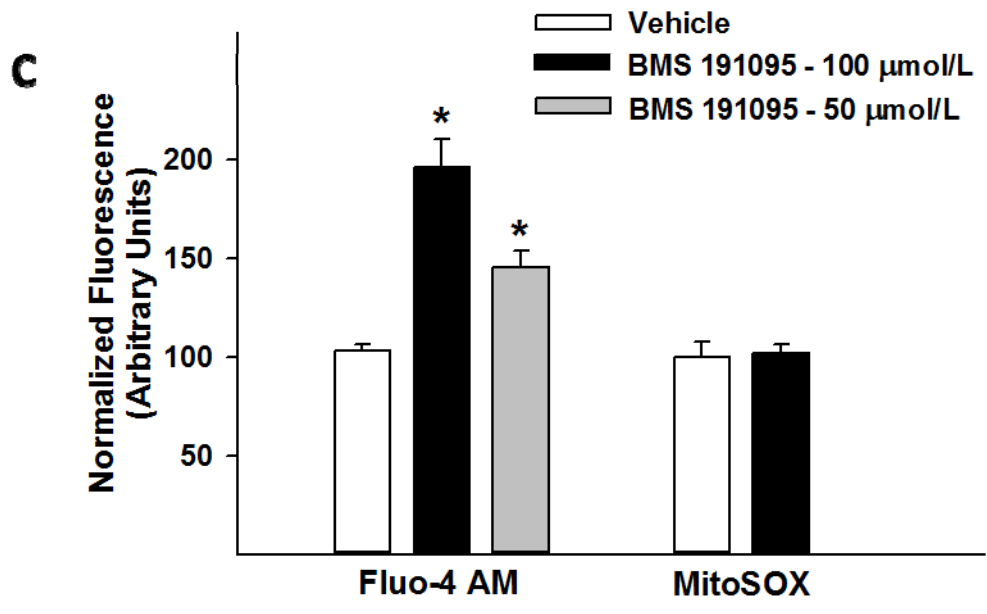
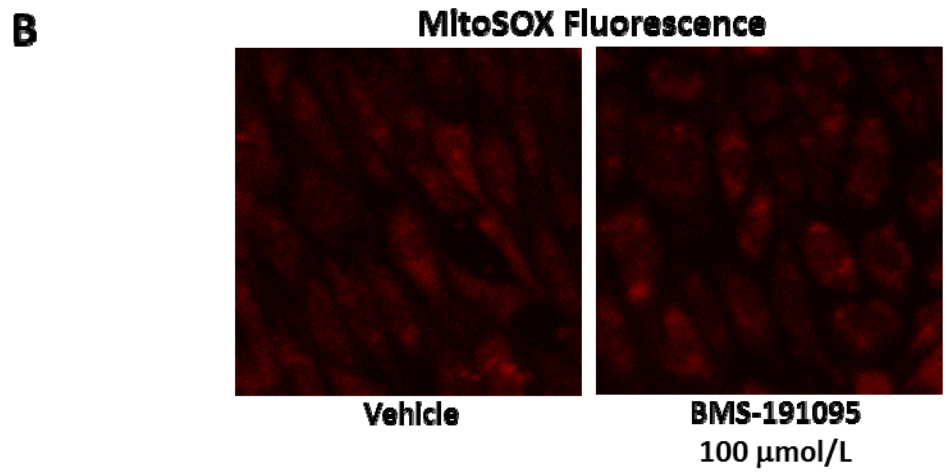
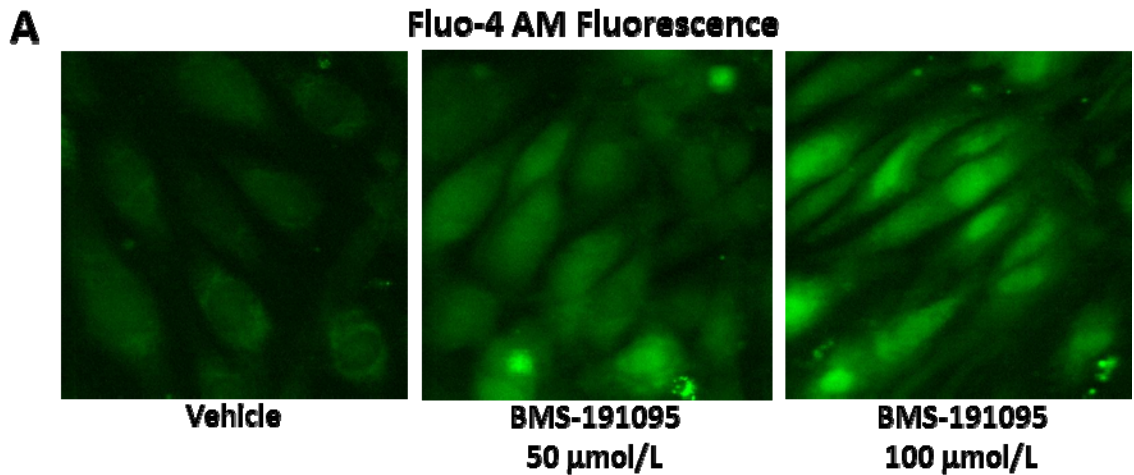


**Figure II.** Fluorescence images of CMVECs loaded with various fluorescent probes and treated with vehicle (DMSO) or 50  $\mu\text{mol/L}$  and 100  $\mu\text{mol/L}$  BMS. Fluorescence images of CMVECs loaded with fluo-4 AM, fluoroprobe for calcium, are shown in panel A. Fluorescence images of MitoSOX, a mitochondrial ROS sensitive dye, are shown in panel B. The cumulative data of fluorescence intensity from the images were determined and plotted as a bar graph for Fluo-4 AM and MitoSOX in panel C. (\*) indicates significant difference in response versus vehicle for corresponding fluorescent probes ( $p < 0.05$ ). BMS promoted dose-dependent increase in fluo-4 AM fluorescence compared with vehicle treated cells indicating elevation of intracellular  $\text{Ca}^{2+}$ . However, BMS treatment even at 100  $\mu\text{mol/L}$  concentration fail to increase MitoSOX fluorescence in endothelial cells compared with vehicle treated cells.

Thus, it appears that even though diazoxide and 100  $\mu\text{mol/L}$  BMS elevate intracellular  $\text{Ca}^{2+}$  to a similar degree, diazoxide promoted mitochondrial ROS elevation in endothelial cells whereas BMS did not. Mitochondrial ROS generation may be triggered by both mitochondrial  $\text{Ca}^{2+}$ -dependent and -independent pathways. This elevation of mitochondrial  $\text{Ca}^{2+}$  in response to increase in intracellular  $\text{Ca}^{2+}$  by BMS may not be sufficient to induce detectable mitochondrial ROS generation in endothelial cells. Alternatively, BMS may have a different impact on mitochondrial  $\text{Ca}^{2+}$  uptake compared with diazoxide, which may explain the differences in the mitochondrial ROS generation in BMS and diazoxide treated cells.



# Depolarization of Mitochondria in Endothelial Cells Promotes Cerebral Artery Vasodilation by Activation of Nitric Oxide Synthase

Prasad V.G. Katakam,<sup>1,2</sup> Edina Wappler,<sup>1,2</sup> Paige Katz,<sup>1</sup> Ibolya Rutkai,<sup>1</sup> Adam Institoris,<sup>2,3</sup> Ferenc Domoki,<sup>2,3</sup> Tamás Gáspár,<sup>2</sup> Samuel M. Grovenburg,<sup>1</sup> James A. Snipes,<sup>2</sup> and David W. Busija<sup>1,2</sup>.

<sup>1</sup>Department of Pharmacology, Tulane University School of Medicine, New Orleans, Louisiana;

<sup>2</sup>Department of Physiology and Pharmacology, Wake Forest University Health Sciences, Winston Salem, North Carolina; <sup>3</sup>Department of Physiology, University of Szeged School of Medicine, Szeged, Hungary.

## MATERIALS AND METHODS

The animal protocol was approved by the Institutional Animal Care and Use Committees of Wake Forest University Health Sciences and Tulane University School of Medicine. The investigation complies with the Guide for the Care and Use of Laboratory Animals published by the US National Institutes of Health. <sup>1</sup> Young, male Sprague Dawley rats (SD, n=32) were obtained at ten weeks of age for vascular experiments and two week old SD rats (n=50) were obtained for cell culture studies. Rats were housed in the animal care facility and received standard rat chow and tap water ad libitum. A detailed description of methods has been provided in the data supplement placed on the journal website.

**Vascular Reactivity.** Rats were sacrificed under deep isoflurane inhalation anesthesia, decapitated and rat brains were isolated. Subsequently, the posterior cerebral arteries were

isolated and vasoreactivity was determined by measuring intraluminal diameter (Living Systems Instrumentation, Burlington, VT) as described previously.<sup>2,3</sup> Briefly, arteries were transferred to a vessel bath filled with oxygenated, warm, physiological salt solution (PSS), cannulated with glass pipettes and secured with nylon thread. Arteries were slowly pressurized with PSS until they developed a stable myogenic tone and cumulative concentration responses to drugs were determined. Endothelium was removed by injecting a bolus of 1 ml of air through the arteries and endothelial denudation was verified by lack of a response to bradykinin.

Vascular responses to BMS (10, 50, and 100  $\mu\text{mol/L}$ ) or diazoxide (10, 50, and 100  $\mu\text{mol/L}$ ) were determined in both endothelium intact and denuded arteries. In addition, responses to 50  $\mu\text{mol/L}$  of BMS or diazoxide were evaluated in endothelium-intact arteries pretreated with manganese(III) tetrakis(4-benzoic acid)porphyrin chloride (MnTBAP, a SOD mimetic, 100  $\mu\text{mol/L}$ ), 5-hydroxydeconic acid (5-HD, 1  $\text{mmol/L}$ , a relatively selective inhibitor of mitoK<sub>ATP</sub> channels), fluoxetine (an inhibitor of mitoK<sub>ATP</sub> channels<sup>4</sup>, 5  $\mu\text{mol/L}$ ), glibenclamide (10  $\mu\text{mol/L}$ , a non-isoform specific K<sub>ATP</sub> channel blocker), wortmannin (a PI3K inhibitor, 100  $\text{nmol/L}$ ), or N<sup>o</sup>-nitro L-arginine methyl ester (L-NAME, a non-isoform selective NOS inhibitor, 100  $\mu\text{mol/L}$ ).

**Endothelial cell cultures.** To evaluate the ability of mitochondrial depolarization to regulate endothelial factors, we determined mitochondrial membrane potential, mitochondrial ROS, NO, and intracellular [Ca<sup>2+</sup>]<sub>i</sub> levels in cultured primary rat brain microvascular endothelial cells (CMVECs). As described previously,<sup>5,6</sup> cortical microvessels were isolated and CMVECs were prepared from the brain cortices of two weeks old rats. Briefly, rats were decapitated under deep anesthesia and the brain cortices were freed from meninges, homogenized, and digested with DNase and collagenase. The homogenate was then centrifuged at 500 g for eight min at 4

°C. Subsequently, the supernatant was collected and redistributed in 20% bovine serum albumin (BSA), and was centrifuged at 1000 g for 20 min at 4 °C to yield cortical microvessels. The microvessels were washed in DMEM, further digested, layered on a continuous 33% Percoll gradient and centrifuged again at 1000 g for ten min at 4 °C. The band of CMVECs were seeded onto collagen IV and fibronectin-coated glass bottom 35mm culture dishes (MatTek, Ashland, MA, USA) and grown until confluent [5-6 d in vitro (DIV)].

**Fluorescence Confocal Microscopy.** Stock solutions of fluoroprobes were prepared in dimethyl sulfoxide, (DMSO). Mitochondrial membrane potential was determined by using rhodamine 123, ( $\lambda_{ex}$ : 488 nm,  $\lambda_{em}$ : >505 nm long pass filter). MitoSOX ( $\lambda_{ex}$ : 405 nm,  $\lambda_{em}$ : >560 nm long pass filter) was used to measure mitochondrial ROS, specifically superoxide, based on the method reported by Robinson et al.<sup>7</sup> Fluo- 4 acetoxymethyl ester (Fluo-4 AM,  $\lambda_{ex}$ : 488 nm,  $\lambda_{em}$ : 505 nm long pass filter) was used to study  $[Ca^{2+}]_i$ , and 4-amino-5-methylamino-2',7'-difluorofluorescein diacetate (DAF-FM,  $\lambda_{ex}$ : 488 nm,  $\lambda_{em}$ : >505 nm long pass filter) was used to measure NO. The CMVECs were loaded in the dark with a 1:1 mixture of 5 $\mu$ mol/L fluo-4 AM or 5 $\mu$ mol/L DAF-FM and 20% (w/v) pluronic F-127 diluted in PBS containing glucose (1g/L) for 30 min at room temperature. For  $[Ca^{2+}]_i$  measurements in arterial endothelial cells, freshly isolated arteries were cut longitudinally, and pinned to a Sylgard block under minimal stretch (tone) with the endothelium facing up using the method described previously.<sup>8</sup> Subsequently, fluo-4 AM was loaded, as described above. MitoSOX ( 5 $\mu$ mol/L) or rhodamine 123 (5  $\mu$ g/ml) solutions were prepared in phenol-free DMEM and CMVECs were loaded with fluoroprobes for 15 min at 37°C. Confocal microscopy was performed using a laser scanning confocal system (LSM 510 and 7 Live; Zeiss, Jena, Germany) attached to an inverted microscope with a Zeiss C-Apochromat 63X /NA 1.2 water immersion objective. MitoSOX

fluorescence was determined by Leica SP2 AOB laser confocal microscope. Fluorescence images were acquired both before and after application of vehicle (DMSO) or BMS (50  $\mu\text{mol/L}$  or 100  $\mu\text{mol/L}$ ) or diazoxide (100  $\mu\text{mol/L}$ ) for rhodamine 123, fluo-4 AM and MitoSOX whereas DAF-FM images were acquired with or without a 30 min L-NAME pretreatment of cells. Imaging conditions such as gain levels and laser power were held constant. Offline analysis of images to determine the average pixel intensity of endothelial cells in each field (n=20-30) was performed using ImageJ software (National Institute of Health, Bethesda, MD) and the results were expressed in relative fluorescence units as % change from the baseline images prior to administration of vehicle, BMS, or diazoxide. The 'n' value represents average fluorescence intensity of all the cells from 'n' number of cover slips that were treated with each treatment.

**NO measurements.** A stock solution of colloid iron diethyldithiocarbamate,  $\text{Fe}^{2+}(\text{DETC})_2$ , was freshly prepared by adding iron sulfate and DETC solutions as described previously.<sup>9, 10</sup> Aortic ring segments were loaded with  $\text{Fe}^{2+}(\text{DETC})_2$  solution (0.4 mmol/L) and treated with vehicle (DMSO), BMS (50  $\mu\text{mol/L}$ ), diazoxide (100  $\mu\text{mol/L}$ ) or spermine NONOate [10  $\mu\text{mol/L}$ , N-(2-Aminoethyl)-N-(2-hydroxy-2-nitrosohydrazino)-1,2-ethylenediamine] in a treatment chamber (Noxygen, Elzach, Germany) at 37 °C for one h. Later, aortic segments were transferred to a liquid nitrogen filled, custom built dewar for NO measurements utilizing electron spin resonance (ESR) spectrometer (e-scan, Bruker Biospin GmbH, Rheinstetten, Germany) with the following settings: microwave power, 40 mW; modulation amplitude, 8G; center field, 2.03 g; sweep width, 80 G; conversion time, 80 msec; time constant, 20 msec; number of scans, 60; sweep time, 10.24 sec. The amount of NO was determined by measuring the total amplitude of the ESR signal for each treatment and comparing it with the ESR signal amplitude of the signal

following NO-donor spermine NONOate. Finally, diazoxide and BMS induced NO production in aortas is expressed as % change from basal levels (vehicle treated).

**Mitochondria and Vascular Signaling.** The CMVECs were treated with vehicle (DMSO), 25  $\mu\text{mol/L}$  BMS, or with diazoxide (100  $\mu\text{mol/L}$ ) in low glucose DMEM medium at 37°C for 15-20 min. Similarly, isolated cerebral arteries were treated with vehicle (DMSO), 50  $\mu\text{mol/L}$  BMS, or with diazoxide (100  $\mu\text{mol/L}$ ). In addition, to evaluate the role of the PI3K pathway, arteries and CMVECs were treated with either vehicle or 100  $\mu\text{mol/L}$  diazoxide, with and without 100 nmol/L wortmannin, in low glucose DMEM medium at 37°C for 15-20 min. Cells and arteries were washed and snap frozen in liquid nitrogen. Subsequently, homogenates were prepared from the cells to determine the cellular signaling by western blotting.

**Western Blot Analysis.** Western blot analyses were performed as previously described.<sup>3</sup> Briefly, equal amounts of extracted protein from homogenates of cerebral arteries or CMVECs were separated by 4-20% SDS-PAGE and transferred onto a nitrocellulose membrane (BioRad). Membranes were blocked with 1% non-fat milk in Tris-buffered saline and 0.05% Tween-20 for 1 h at room temperature. Subsequently, the membranes were incubated overnight at 4 °C with the primary antibodies for total eNOS and protein kinase B (Akt) (1:4000; BD Transduction laboratories) and phosphorylated eNOS (Ser1177) and Akt (Ser473) (1:2000; Cell Signaling Technology, Inc.), and  $\beta$ -actin (1:2500; Sigma). The membranes were then washed for 2 h in the blocking buffer with anti-rabbit IgG (1:10,000 dilution; Jackson ImmunoResearch) conjugated to horseradish peroxidase. The final reaction products were visualized using enhanced chemiluminescence (SuperSignal West Pico; Pierce, Rockford, IL, USA) and recorded on X-ray film. Western blots were analyzed as the immunoband intensity ratio of phosphorylate to the corresponding total eNOS or Akt.



**Drugs, chemicals and solutions.** All chemicals were purchased from Sigma (St. Louis, MO, USA) except MnTBAP (Calbiochem, San Diego, CA), DETC (Noxygen, Elzach, Germany) rhodamine 123, MitoSOX, DAF-FM, fluo-4 AM, Pluronic F-127 (Molecular Probes, Eugene, OR), DMEM (Gibco BRL, Grand Island, NY, USA), fetal bovine plasma-derived serum (Animal Technologies, Tyler, TX), and Percoll (Amersham Biosciences, Uppsala, Sweden).

**Data analysis and statistics.** Results were expressed as mean±SEM; 'n' indicates the number of independent experiments. Means were compared by one-way ANOVA. Post-hoc analysis was done by Tukey's test. A p<0.05 was considered as statistically significant.

## REFERENCES

1. National Guide for the Care and Use of Laboratory Animals (8th Edition): National Research Council (US) Committee for the Update of the Guide for the Care and Use of Laboratory Animals. *National Academies Press (US)*. 2011;NIH Publication 85-23.
2. Busija DW, Katakam P, Rajapakse NC, Kis B, Grover G, Domoki F, Bari F. Effects of ATP-sensitive potassium channel activators diazoxide and BMS-191095 on membrane potential and reactive oxygen species production in isolated piglet mitochondria. *Brain Res Bull.* 2005;66:85-90.
3. Katakam PV, Domoki F, Snipes JA, Busija AR, Jarajapu YP, Busija DW. Impaired mitochondria-dependent vasodilation in cerebral arteries of Zucker obese rats with insulin resistance. *Am J Physiol Regul Integr Comp Physiol.* 2009;296:R289-298.
4. Wojtovich AP, Williams DM, Karcz MK, Lopes CM, Gray DA, Nehrke KW, Brookes PS. A novel mitochondrial K(ATP) channel assay. *Circ Res.* 2010;106:1190-1196.

5. Perriere N, Demeuse P, Garcia E, Regina A, Debray M, Andreux JP, Couvreur P, Scherrmann JM, Tamsamani J, Couraud PO, Deli MA, Roux F. Puromycin-based purification of rat brain capillary endothelial cell cultures. Effect on the expression of blood-brain barrier-specific properties. *J Neurochem.* 2005;93:279-289.
6. Katakam PV, Domoki F, Lenti L, Gaspar T, Institoris A, Snipes JA, Busija DW. Cerebrovascular responses to insulin in rats. *J Cereb Blood Flow Metab.* 2009;29:1955-1967.
7. Robinson KM, Janes MS, Beckman JS. The selective detection of mitochondrial superoxide by live cell imaging. *Nat Protoc.* 2008;3:941-947.
8. Ledoux J, Taylor MS, Bonev AD, Hannah RM, Solodushko V, Shui B, Tallini Y, Kotlikoff MI, Nelson MT. Functional architecture of inositol 1,4,5-trisphosphate signaling in restricted spaces of myoendothelial projections. *Proc Natl Acad Sci U S A.* 2008;105:9627-9632.
9. Fink B, Dikalov S, Fink N. ESR techniques for the detection of nitric oxide in vivo as an index of endothelial function. *Pharmacol Rep.* 2006;58 Suppl:8-15.
10. Cai H, Li Z, Dikalov S, Holland SM, Hwang J, Jo H, Dudley SC, Jr., Harrison DG. NAD(P)H oxidase-derived hydrogen peroxide mediates endothelial nitric oxide production in response to angiotensin II. *J Biol Chem.* 2002;277:48311-48317.